Slip partitioning at convergent plate boundaries of SE Asia

Robert McCaffrey

Geological Society, London, Special Publications 1996; v. 106; p. 3-18
doi: 10.1144/GSL.SP.1996.106.01.02

Slip partitioning at convergent plate boundaries of SE Asia

ROBERT McCAFFREY
Department of Earth & Environmental Sciences, Rensselaer Polytechnic Institute, Troy, New York 12180, USA

Abstract: The active tectonics of SE Asia can be characterized by the interactions of large, rigid plates separated by broad zones of deformation. The relative motion of these plates across their boundaries is often partitioned in the sense that the normal and shear components occur on different structures. Earthquake slip vectors and geological and geodetic measurements are used to infer the degree to which oblique convergence, which is ubiquitous in SE Asia, is partitioned. The active tectonics of Sumatra, the Himalayan thrust, the Philippines, the New Guinea fold-and-thrust belt, the Huon–Finisterre collision, and the San Cristobal trench can be understood in terms of upper plate deformation associated with oblique convergence. Western Java may also exhibit partitioning of oblique subduction. Structures accommodating normal and shear components of the motion are often very close. Arc-parallel strain rates are estimated for forearcs of the region. The arc-parallel deformation of forearcs of the SE Asia region demonstrates that plate convergence, whether normal to structure or not, is a three-dimensional process.

When convergence between two plates is not perpendicular to their boundary, shear stress parallel to the plate boundary results in margin-parallel shear strain within both plates. In a collision belt or subduction zone, if one of the plates is weak in shear, then the total slip may be partitioned into shear and thrust components (defined by the plate boundary orientation). Often these shear and normal components of slip across the boundary are accommodated on different geological structures. Oblique convergence is globally much more common than trench-normal convergence and often the obliquity varies along the margin. The deformation in many convergence zones may be understood in terms of such slip partitioning. A widely cited example of these parallel structures is along the San Andreas system, which comprises a strike-slip fault and a parallel fold-and-thrust belt (Mount & Suppe 1987) even though the relative motion between the Pacific and North American plates is only a few degrees from the trend of the San Andreas fault.

Throughout SE Asia and the SW Pacific, we see several examples of oblique convergence (Fig. 1), both in subduction and collision settings. Studies of Sumatra led Fitch (1972) to first propose that slip was sometimes accommodated by parallel thrust and strike-slip faults. Since that study, it has been found that partitioning of oblique subduction is globally quite common although it is rarely completely partitioned (Jarrard 1986; McCaffrey 1994). Similar geometries, in which a major strike-slip fault accommodates the boundary-parallel shear strain, exist in the Philippines (Barrier *et al.* 1991) and possibly in Irian Jaya (Abers & McCaffrey 1988). Other convergence zones that have clear slip partitioning are the Himalayan thrust (Molnar & Lyon-Caen 1989), the Aegean (Gilbert *et al.* 1994), New Zealand (Anderson *et al.* 1993) and the Aleutians (Ekström & Engdahl 1989; McCaffrey 1992). McKenzie & Jackson (1983) argued that, if plate motions are driven by ductile shear from below, oblique convergence in continental settings should be completely partitioned, that is, slip will occur only on strike-slip and pure thrust faults. This theory provides a test of crustal dynamics in oblique collision zones but requires detailed knowledge of the deformation. SE Asia is a good region to test such ideas because oblique convergence zones are plentiful and fast.

In the past few years much has been done to improve our knowledge of the patterns of crustal deformation in SE Asia. In particular, systematic studies of large earthquakes, geological studies of active faults, and geodetic measurements using the Global Positioning System (GPS), that commenced in the SW Pacific region in 1988, are revealing important results, and surprises. The goal of this paper is to review our knowledge of the crustal deformation in SE Asia with attention to the partitioning of slip between thrust and shear faults in the broad deforming boundaries. First, constraints on the motions of the major plates are discussed in order to put bounds on the convergence geometries and then the deformation within these zones is described.

From Hall, R. & Blundell, D. (eds), 1996, *Tectonic Evolution of Southeast Asia*, Geological Society Special Publication No. 106, pp. 3–18.

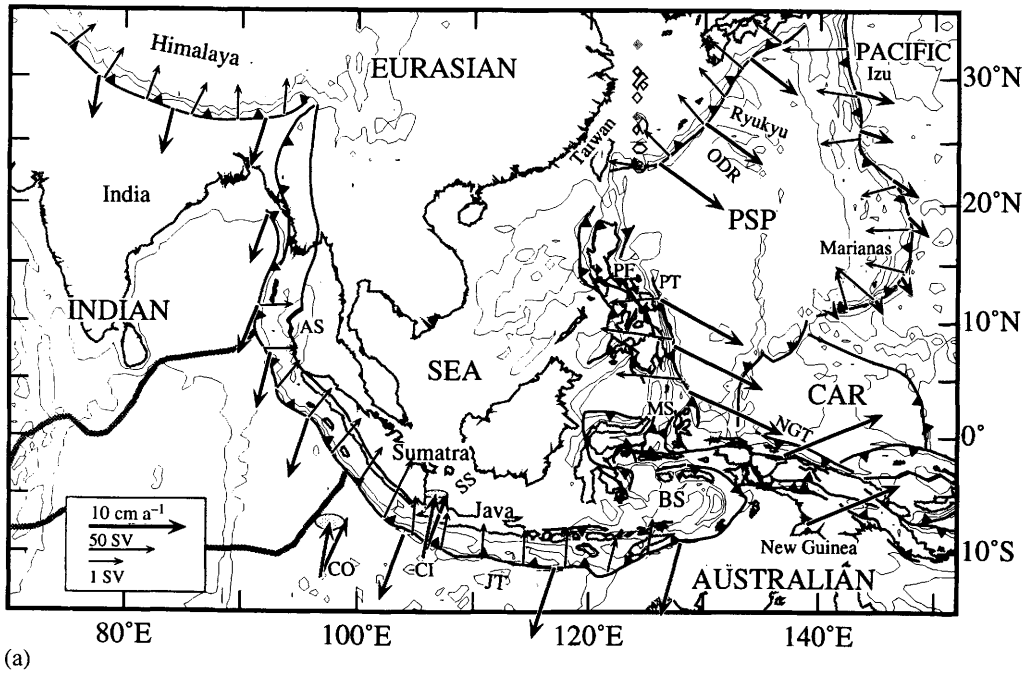
Himalaya
EURASIAN
PACIFIC
Izu
India
Taiwan
Ryukyu
ODR
PSP
Marianas
PF
PT
INDIAN
AS
SEA
CAR
MS
NGT
Sumatra
SS
Java
BS
New Guinea
10 cm a-1
50 SV
1 SV
CO
CI
JT
AUSTRALIAN
30°N
20°N
10°N
0°
10°S
80°E
100°E
120°E
140°E

(a)

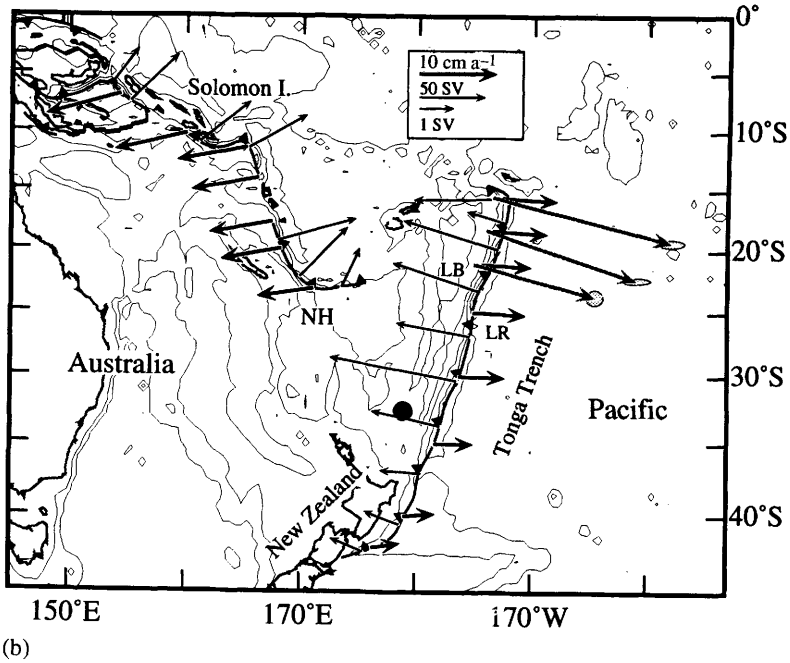
10 cm a-1
50 SV
1 SV
Solomon I.
LB
NH
LR
Australia
Tonga Trench
Pacific
New Zealand
0°
10°S
20°S
30°S
40°S
150°E
170°E
170°W

(b)

Plate motions

The broad kinematic framework of SE Asia, determined by the relative motions of the Pacific, Australian, and Eurasian plates, is described to the first order by NUVEL-1A, the global plate motion solution of DeMets *et al.* (1994*a*). In addition, the motions of the Philippine Sea, the SE Asian, and Caroline plates control the large-scale tectonics of the region, and these are discussed below.

SE Asia as a separate plate

One of the important regional problems is whether or not SE Asia (SEA) moves independently of Eurasia. This question is linked to collision in the Himalayan region and its answer will provide constraints on the mechanism of continental collision. Recently, the first direct measurements of the relative motion between Australia and Indonesia across the Java trench were made. Five GPS measurements over 4 years on a baseline between Christmas Island (Fig. 1a) and western Java reveal a relative velocity (67 ± 7 mm a^{-1} rate at $011 \pm 4°$ azimuth) that matches the NUVEL-1A vector for Australia relative to Eurasia (71 ± 2 mm a^{-1} rate at $020 \pm 3°$ azimuth) within 1 cm a^{-1} (Tregoning *et al.* 1994) (Fig. 1a). This single vector can be interpreted in several ways: that SEA moves slowly if at all relative to Eurasia (within the uncertainties of GPS); that SEA moves relative to Eurasia but the pole of rotation is near western Java; or that elastic strains contaminate the geodetic signal due to the proximity of the GPS sites to the plate boundary. Until more results become available, the author favours the first view – that SEA moves very slowly, 1 cm a^{-1} or less, northward relative to Eurasia. Because the motion of SEA relative to Eurasia is slow and the pole of rotation is poorly constrained, in the following discussions SEA will be treated as part of Eurasia.

The Philippine Sea plate

The motion of the Philippine Sea plate (PSP) is still poorly constrained due to lack of reliable kinematic data; only subduction zone earthquake slip vectors are available (Ranken *et al.* 1984; Seno *et al.* 1993) and these are probably deflected by local deformation of the leading edges of the upper plates (McCaffrey 1994). Moreover, earthquake slip vectors do not contain information about rates of motion.

Despite these handicaps, Seno *et al.* (1993) revised estimates of PSP motion by constraining it to comply with the NUVEL-1A global solution. However, this does not improve the tie of the PSP to its neighbouring plates; for example the uncertainty in the latitude of the Pacific–PSP pole is nearly 50° (Seno *et al.* 1993). Ongoing programmes by several groups to measure the motion and deformations of the PSP with GPS will provide the required data to constrain the PSP motion relative to the rest of the world. Recent GPS measurements across Taiwan (Yu & Chen 1994) show that the PSP and Eurasia converge at azimuth $307° \pm 1$ and a rate of 86 ± 2 mm a^{-1}, which is in a similar direction but 20% faster than the Seno *et al.* (1993) PSP–Eurasia pole predicts. A very long baseline interferometry vector (Matsuzaka *et al.* 1991) between sites on Japan (North American plate) and the Izu-Bonin arc (PSP) also agrees with the azimuth predicted by the combined PSP–North America Euler pole (Seno *et al.* 1993; DeMets *et al.* 1994*a*) but is 15% faster. Both results suggest that Seno *et al.* may have underestimated the angular velocities for the PSP relative to Eurasia and North America. In the following, the Seno *et al.* (1993) poles are used for the PSP but other poles are tried in the kinematic analyses of forearcs around the PSP.

The Caroline plate

Weissel & Anderson (1978) argued for the existence of a separate Caroline plate (CAR)

Fig. 1. Tectonic maps. (**a**) SE Asia. Thrust faults have barbs on the hanging wall. Heavy black arrows show relative plate motions at boundaries (vectors show upper plate moving relative to lower) using poles given in Table 1. Grey arrows with error ellipses show GPS vectors of Cocos Island (CO) and Christmas Island (CI) relative to Java (Tregoning *et al.* 1994) (black arrows show expected Australia–Eurasia vector). Small arrows pointing landward of trenches show average slip vector (SV) azimuths of interplate thrust earthquakes along 400 km long segments of the forearcs (lengths of arrows are scaled to number of SV in average). Thick grey lines show outline of broad deforming region between the Indian and Australian plates (DeMets *et al.* 1994*b*). SEA, SE Asian plate; PSP, Philippine Sea plate; ODR, Oki Daito ridge; CAR, Caroline plate; JT, Java trench; BS, Banda Sea; MS, Molucca Sea; PF, Philippine fault; PT, Philippine trench; AS, Andaman Sea; SS, Sunda Strait; NGT, New Guinea trench. Bathymetry contours at 2000 m intervals. (**b**) Southwest Pacific. Format same as (a). GPS vectors are relative to Pacific plate (Bevis *et al.* 1995). The large dot north of New Zealand is the pole of rotation of the N. Tonga forearc relative to the Pacific determined from GPS vectors. NH, New Hebrides arc; LB, Lau Basin; LR, Louisville Ridge; SV, slip vector.

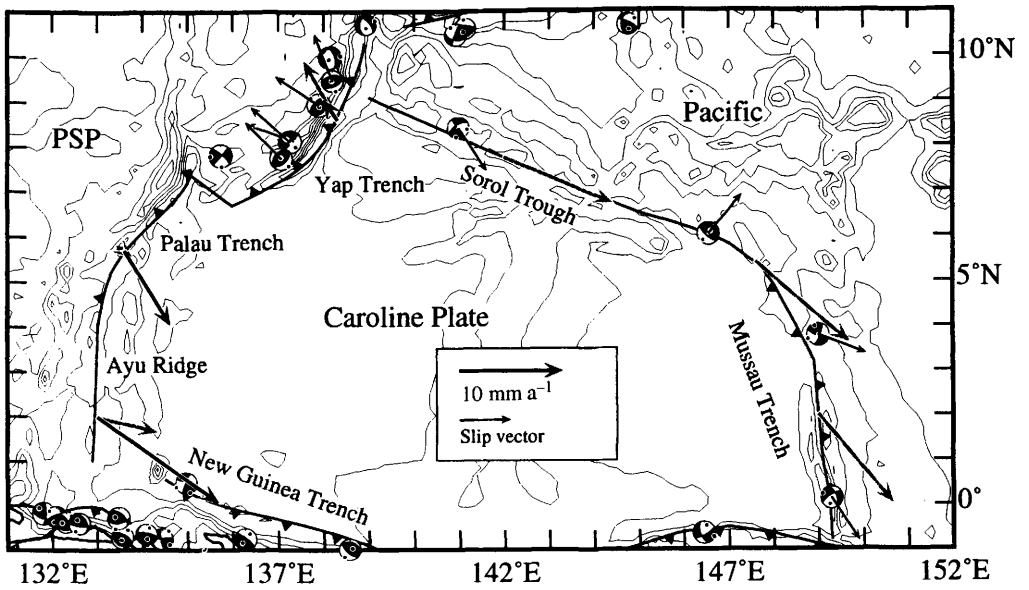

Fig. 2. Plot of bathymetry, plate boundaries, relative plate motion vectors (thick arrows), and earthquake mechanisms and slip vectors (thin black arrows) around the Caroline plate. Grey arrows show the expected motion of the Caroline plate relative to the Pacific and Philippine Sea (PSP) plates and the thicker black arrows show the motion of the Pacific relative to the PSP, all based on the Seno *et al.* (1993) poles. Earthquake mechanisms are from the Harvard CMT catalogue. PSP, Philippine Sea plate.

between the Pacific, the PSP, and northern New Guinea (Fig. 1a). This suggestion was based largely on the morphologies of the Mussau trench and Sorol trough (Fig. 2); the former thought to be a subduction zone and the latter predominantly a left-lateral shear zone with some extension. Rates of motion of CAR relative to surrounding plates are based on the observed increase in sediment thickness away from the Ayu Ridge (Weissel & Anderson 1978) and on inferences about the amount of shortening at the Mussau trench (Hegarty *et al.* 1983). Such motions are estimated at less than 1 cm a^{-1}.

Ranken *et al.* (1984) and Seno *et al.* (1993) estimated rotation poles for CAR relative to the Pacific and PSP by requiring convergence along the Mussau trench and a combination of extension and strike-slip at the Sorol trough. Recent earthquake mechanisms along the Mussau trench and Sorol trough (Fig. 2) are not consistent with a simple plate boundary between CAR and the Pacific. The slip vector for one event near the intersection of the Sorol trough and Mussau trench is nearly orthogonal to the expected slip based on the Seno *et al.* Pacific–CAR pole. Events along the Mussau trench itself indicate some thrusting but mostly right-lateral strike-slip on very steep planes that are consistent with the strike and polarity of the trench. Thrust earthquakes along the Yap trench have slip vectors that are consistent with either Pacific–PSP or CAR–PSP motion. The alleged Caroline–Pacific plate boundary is not a very compelling feature and may simply be a region where stress concentrates due to locally steep, inherited topography. In this paper it is presumed that the 'Caroline plate' is kinematically part of the Pacific plate. Even if the Caroline plate is a separate block, ignoring it in the kinematic analysis will not be critical because it probably moves slowly relative to surrounding plates.

Deforming boundary zones and slip partitioning

By far the most elusive aspect of SE Asian tectonics is the description of the deforming zones between the rigid portions of the major plates described above. One way to view the deformation of the plate boundary zones is in terms of slip partitioning. Before discussing slip partitioning at convergent margins of SE Asia, some basic geometrical concepts are reviewed. The mechanics of slip partitioning are discussed by McCaffrey (1992) and Platt (1993) but this paper concentrates on the kinematic consequences. Most of the inferences

drawn here are based on the deflections of slip vectors of interplate earthquakes away from the expected convergence direction between the two plates (Fig. 1 shows orientations of slip vectors and plate vectors along plate boundaries). Earthquake slip vector deflections tell us mostly about the arc-parallel component of deformation within the upper plate, because most convergence is at a high angle to the trench normal, arc-normal deformation of the forearc does little to deflect the slip vectors (McCaffrey 1991). If the plate convergence vector and the orientation of the trench are known, then the arc-parallel rate of motion v_s of the forearc relative to the upper plate can be inferred from the slip vector based on a simple kinematic relationship (Fig. 3). Moreover, if the obliquity varies along the margin then v_s may vary as well, resulting in an arc-parallel strain rate. Note that the arc-parallel strain rate arises from the gradient in obliquity, not from the obliquity itself, and we will see that arc-parallel strain can occur where the obliquity is zero. Hence, even though subduction may be locally perpendicular to the trench and apparently two-dimensional, rapid arc-parallel deformation of the upper plate can occur, producing a three-dimensional strain field.

Earthquakes used are those that reveal slip between the subducting plate and the overriding forearc. McCaffrey (1994) discusses the selection of data (i.e. trench orientations, plate convergence vectors and slip vectors) needed for this type of analysis. Slip vectors are averaged in 50–150 km long segments of the trenches. This paper uses the Harvard centroid-moment tensor solutions from 1977 through August 1994 and other published solutions for earthquakes prior to 1977. It is assumed that the downgoing plate does not deform rapidly; slip vector deflections require motions of a large percentage of the plate motion rate and it is unlikely that subducting plates are sheared at such high rates. The goal is to infer arc-parallel slip rates v_s (Fig. 3) and arc-parallel strain rates (arc-parallel gradients in v_s) in forearcs in the SE Asia region (Table 1). Where available the slip vector derived slip rates are compared to geological or geodetic measurements of slip rates.

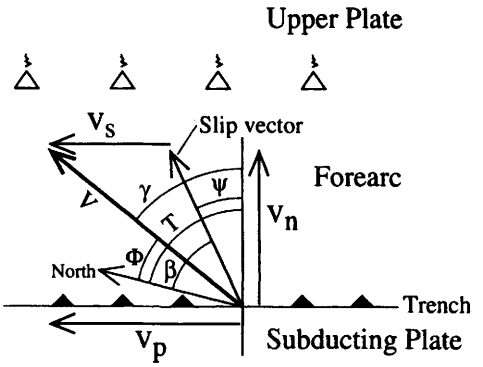

v = predicted plate convergence vector

T = trench-normal azimuth

Φ = plate motion azimuth

β = slip vector azimuth

ψ = trench normal - slip vector = T - β

Obliquity: $\gamma = T - \Phi$

Slip vector residual: $\Delta\beta = \beta - \Phi$

Forearc slip rate relative to Upper Plate:

$v_S = v (\sin\gamma - \cos\gamma \tan\psi)$

Fig. 3. Geometry of slip partitioning as inferred from earthquake slip vectors. The important items are γ, the plate convergence obliquity, ψ, the slip vector obliquity, and v_s, the slip rate of the forearc in the arc-parallel direction relative to the upper plate.

Sumatra and Java

Fitch (1972) correctly inferred that oblique convergence at Sumatra was partitioned into a component of thrusting at the Java trench that was normal to the trench and a component of arc-parallel shear on the Sumatra fault. In the past few years, detailed investigations utilizing more and better data have refined the kinematics of the Sumatra region. Attempts to treat the Sumatra forearc, between the trench and the Sumatra fault, as a rigid plate (e.g. Curray 1989) generally failed to explain subduction west of the Andaman Sea, where the trench takes a turn to the NNE (Fig. 1a) or the difference in the amount of extension in the Sunda Strait (100 km) (Huchon & Le Pichon 1984; Harjono *et al.* 1991) and Andaman Sea (400 km) (Curray *et al.* 1979). These features can be explained if the forearc stretches in addition to being translated northwestward relative to SEA (Diament *et al.* 1990; McCaffrey 1991).

Using a convergence direction at the Java trench of N3°E and a rate of 75 mm a^{-1}, an arc-parallel extensional strain rate of $3–4 \times 10^{-8}$ a^{-1} is required of the Sumatra forearc to match the deflections of the slip vectors (McCaffrey 1991). Tregoning *et al.* (1994) show that the NUVEL-1A Australia–Eurasia vector is approximately correct for the Java trench. The NUVEL-1A Australia-Eurasia convergence direction results in a lower inferred arc-parallel strain rate ($1.8 \pm 0.5 \times 10^{-8}$ a^{-1}; Fig. 4a, Table 1) than the N3°E direction does because it matches better the slip vectors west of Sumatra.

Such arc-parallel stretching of the forearc implies that the slip rate on the Sumatra fault

Table 1. *Arc-parallel strain rates for forearcs*

Trench name	Pole of rotation*	Number of trench segments	Number of slip vectors	Arc-parallel strain rate ($\times 10^{-8}$ a^{-1})	Correlation coefficient	RMS (mm a^{-1})
Himalaya	N IND–EUR	13	19	2.2 ± 0.5	0.79	12
Izu	S PAC–PSP	7	67	0.7 ± 0.7	0.52	6
Java	N AUS–EUR	15	40	–0.1 ± 0.4	–0.05	12
Mariana	S PAC–PSP	10	61	1.7 ± 0.5	0.81	6
New Hebrides	N PAC–AUS	11	124	12.3 ± 2.5	0.96	25
N. Ryukyu	S PSP–EUR	5	27	1.3 ± 0.3	0.92	2
N. Tonga	N PAC–AUS	4	99	16.3 ± 5.4	0.93	14
Philippine	S PSP–EUR	23	140	2.6 ± 1.0	0.60	18
S. Ryukyu	S PSP–EUR	4	14	0.6 ± 1.6	0.13	7
S. Tonga	N PAC–AUS	15	481	–0.1 ± 0.4	0.15	11
Sumatra	N AUS–EUR	18	102	1.8 ± 0.5	0.84	11

* N, Demets *et al.* (1994a) NUVEL-1A; S, Seno *et al.* (1993); IND, India; EUR, Eurasia; PAC, Pacific; PSP, Philippine Sea plate; AUS, Australia.
Trench segments are between 50 and 150 km long.
Positive values of strain rates are arc-parallel extensional, and negative values are compressional.

increases to the NW (McCaffrey 1991), which is supported by the few direct measurements of slip rate on the fault (Fig. 4a). At its southern end, near 5°S, the slip rate is less than 10 mm a^{-1} (Bellier *et al.* 1991) but increases to about 10 mm a^{-1} near the equator and to about 28 mm a^{-1} near 2.2°N (Sieh *et al.* 1994) (Fig. 4a). The average gradient in the slip rate on the fault is close to that predicted from slip vector deflections; an increase in 28 mm a^{-1} over 1200 km from the Sunda Strait to 2.2°N gives a strain rate of 2.3×10^{-8} a^{-1}.

As is seen in Fig. 4a, slip vectors and the NUVEL-1A Australia–Eurasia pole give approximately the correct slip rate for the Sumatra fault but also predict left-lateral, arc-parallel shear at a rate of 15–20 mm a^{-1} at the longitude of W Java. A pole of rotation that fits the earthquake slip vectors south of Java, and hence does not require upper plate deformation near Java, predicts higher than observed slip rates for the Sumatra fault (McCaffrey 1991). Therefore, either the earthquake slip vectors are poor indicators of upper plate deformation, there are faults other than the Sumatra fault that accommodate forearc deformation off Sumatra (Karig *et al.* 1980; Diament *et al.* 1992), or there is left-lateral shear through Java (Dardji *et al.* 1991; Malod *et al.* 1996). The constant v_s value at Java (Fig. 4a) indicates a near-zero strain rate. The Java forearc may be moving relative to the Sunda shelf but, unlike the Sumatra side, not undergoing internal strain.

The mechanism for the arc-parallel stretching of the Sumatra forearc is unclear but involves some extension on cross-forearc faults, such as in the strait between Java and Sumatra (Huchon & Le Pichon 1984; Harjono *et al.* 1991; Malod *et al.* 1996), and some strike-slip faults crossing the forearc (Karig *et al.* 1980). The largest shallow, strike-slip earthquake to occur in Sumatra in the past 30 years was beneath the forearc and had nodal planes

Fig. 4. Plot of plate convergence obliquity (shaded curves), slip vector obliquity (open circles), arc-parallel forearc slip rates (v_s, closed circles), and arc-parallel slip rate of subducting plate (v_p, thin solid curve) along convergence zones of SE Asia. The horizontal axis is distance in kilometres along the deformation front or trench (also labelled with approximate latitude or longitude). Positive distance is the direction faced if the thrust fault dips to the viewer's right (for example, positive distance is west if the fault dips N). The vertical axis is angles in degrees and slip rates in mm a^{-1}. Plate obliquity is inferred from trench-normals, plate convergence directions (poles used are listed in Table 1), and their uncertainties. Thin dashed curves, when present, show obliquity from poles of rotation based on fitting slip vectors at the trench. Slip vector obliquity is the angle between the slip vector and the direction normal to the trench (Fig. 3). Positive values of v_s indicate right-lateral shear and negative values are left-lateral. Heavy dark straight lines show the best-fit to the values of v_s, the slope of which (dv_s/dx) is the arc-parallel strain rate (Table 1; positive slopes show arc-parallel extension, negative slopes show arc-parallel compression). Triangles show geodetic and geological estimates of arc-parallel slip rates, as discussed in text. NZ, New Zealand.

that were rotated by 45° relative to the trend of the Sumatra fault (Zwick & McCaffrey 1991). It is likely that more detailed study of the Sumatra forearc structure will find complex deformation, such as in the Aleutian (Geist *et al.* 1988) and Cascadia (Goldfinger *et al.* 1992) forearcs.

Himalaya

Due to the extensive deformation within Asia north of the Himalaya the convergence rate and direction at the Himalayan front is poorly constrained. The convergence rate is estimated to be 15 mm a^{-1}

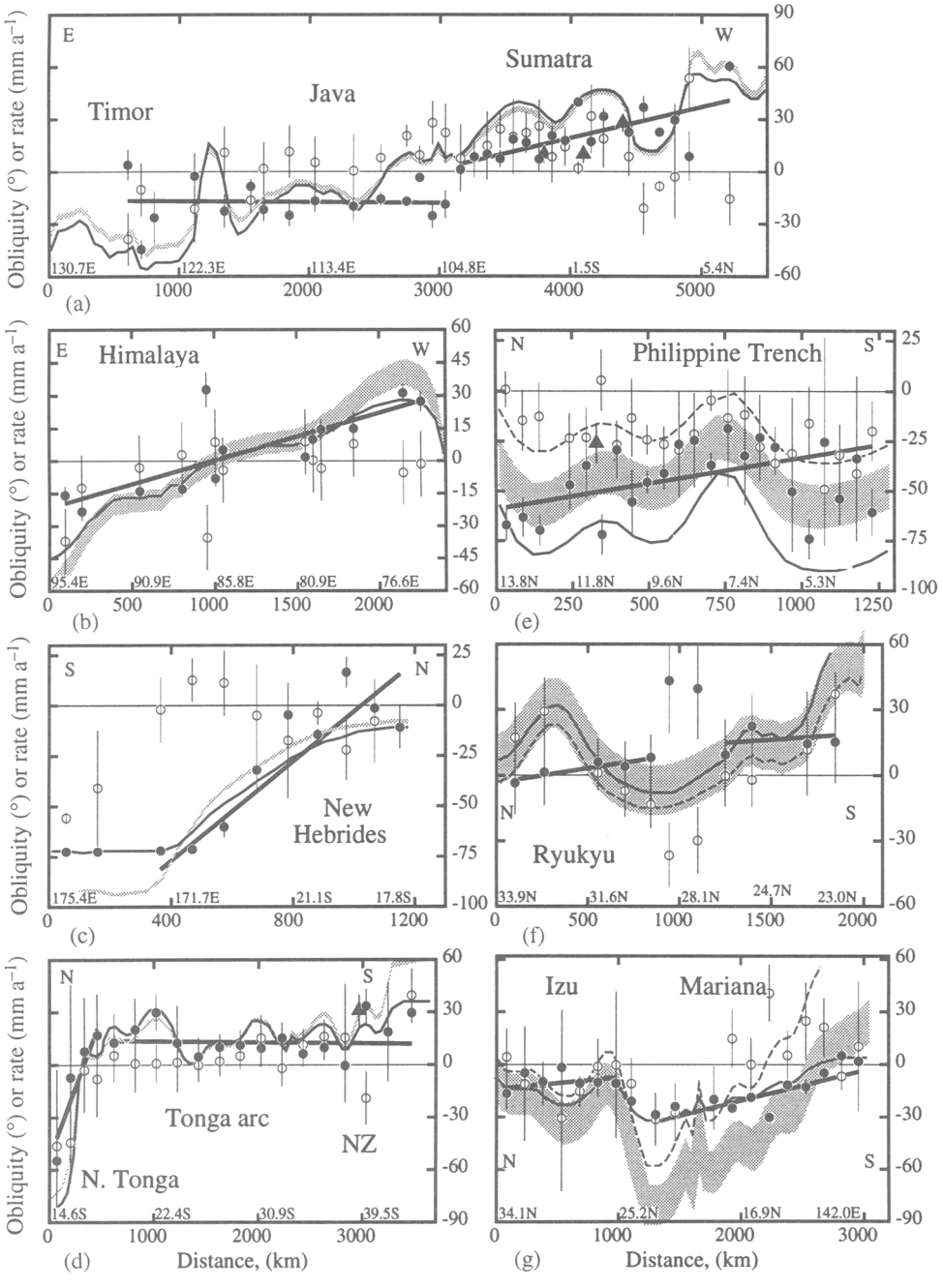

(Molnar & Lyon-Caen 1989), or about one-third of the total India–Eurasia motion. Due to the large curvature of the Himalayan front, the obliquity varies by more than 90° along it (Fig. 4b). Despite this large variation in obliquity, earthquake slip vectors tend to remain perpendicular to the thrust front instead of following the convergence direction (Fig. 4b). Kinematically this requires deformation of the overriding plate. The uniform arc-parallel strain rate estimated from slip vectors

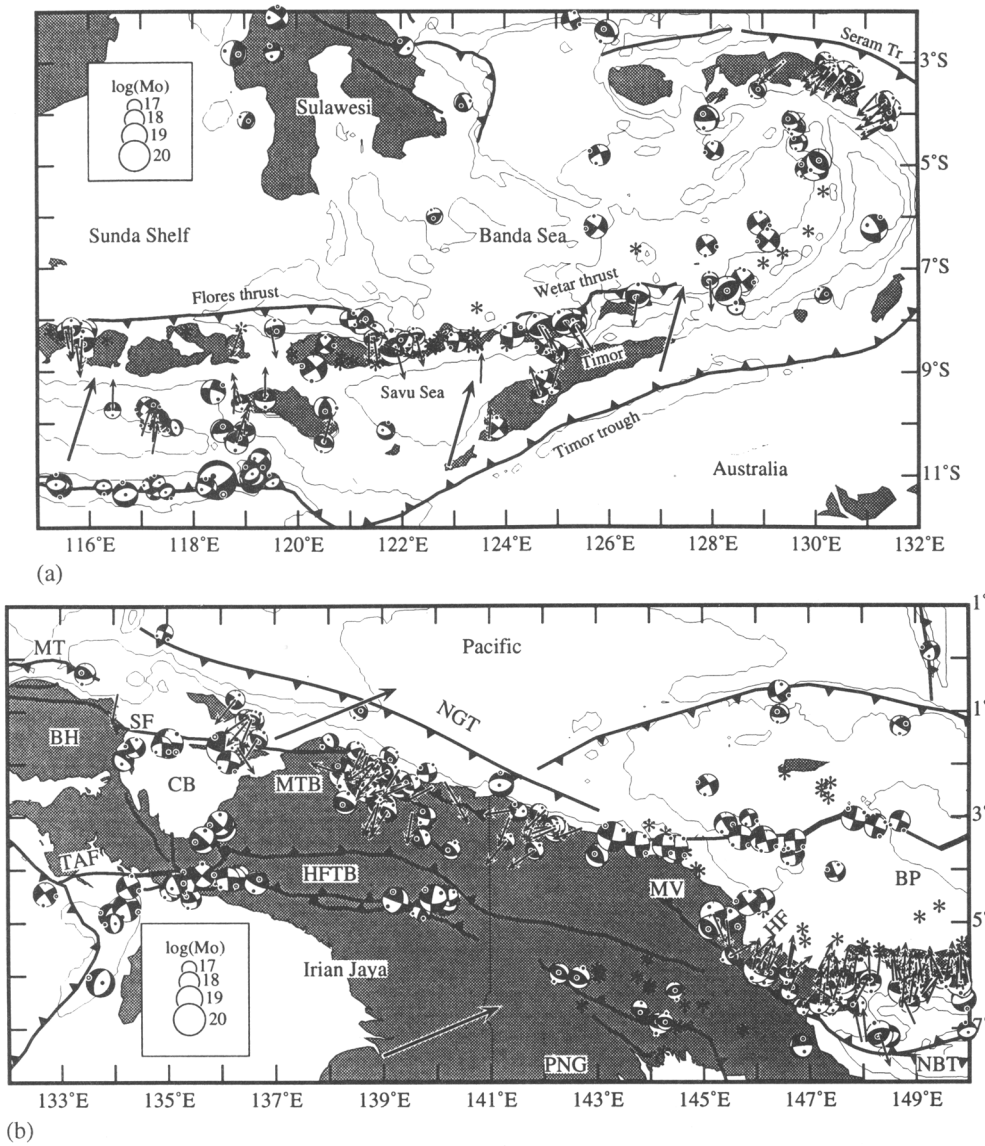

Fig. 5. Fault plane solutions (1962–1984; $M_s \geq 5.5$), slip vectors, and plate vectors for (**a**) eastern Indonesia and (**b**) New Guinea. Size of earthquake symbol is scaled to logarithm of seismic moment. Asterisks show active volcanoes. Small arrows show slip vectors of interplate thrust earthquakes and large arrows show expected plate convergence directions based on (a) Australia–Eurasia and (b) Australia-Pacific (DeMets *et al.* 1994a). MT, Manokwari trough; BH, Bird's Head; SF, Sorong fault; CB, Cenderwasih Bay; TAF, Tarera–Aiduna fault; MTB, Mamberambo thrust belt; HFTB, Highlands fold-thrust belt; NGT, New Guinea trench; MV, Markham Valley; HF, Huon–Finisterre Range; BP, Bismarck plate; NBT, New Britain trench; PNG, Papua New Guinea.

is $2.2 \pm 0.5 \times 10^{-8}$ a^{-1} (Fig. 4a) if the India–Eurasia convergence rate is used and one-third of that (i.e., 0.7×10^{-8} a^{-1}) if two-thirds of India-Eurasia convergence is taken up in Asia. Molnar & Lyon-Caen (1989) estimate $1.0 \pm 0.5 \times 10^{-8}$ a^{-1} (18 ± 9 mm a^{-1} over a distance of 1800 km) for the rate of E–W extension of Tibet.

Extension of the Himalayan frontal arc is thought to be driven by gravitational collapse of the overthickened Tibetan Plateau, instead of shearing due to oblique plate convergence. The evidence for this is the correlation of faulting type with elevation. Normal faulting is confined to elevations above 4000 m, strike-slip occurs at all elevations, and thrust faulting is confined to elevations below 4500 m (e.g. Molnar *et al.* 1993). However, because the earthquakes showing rotated slip vectors occur within 200 km of the thrust front, the Himalayan forearc must also be extending along strike at about 10^{-8} a^{-1}. Therefore, while normal faulting may be confined to high elevations, E–W extension of the upper plate is not. As is the case for the Sumatra forearc, such extension could be accommodated by strike-slip faulting at low elevations instead of normal faulting.

Note that the arc-parallel strain rate applies even to the region near 86°E (≈ km 1000) where subduction is perpendicular to the mountain front. (At several other subduction zones in Fig. 4, similarly, the strain rate is not zero even thought the plate obliquity is near zero.) Even though $v_s \approx 0$, the margin-parallel gradient in v_s is non-zero. In the case of normal convergence, strain will occur in the vertical plane containing the convergence vector and the normal to the margin. Since v_s represents motion perpendicular to this plane, a gradient in v_s results in strain outside of this plane, producing a three-dimensional strain tensor. The force that stretches the forearc along its length arises from the gradient in the arc-parallel shear stress due to the increase in obliquity on both sides of the point where margin-perpendicular convergence occurs (McCaffrey 1992). Hence, subduction at a curved margin is a three-dimensional process even where it may be locally perpendicular to the trench.

Banda arc and Timor

Earthquakes suggest that the present stage of the collision of the Australian continental margin with the Banda arc probably involves more rapid convergence at the backarc thrusts than at the Timor trough (Fig. 5a). The Wetar and Flores backarc thrust zones are considerably more energetic seismically than the subduction thrust fault north of the eastern Java trench and Timor trough (McCaffrey 1988); all known large thrust earthquakes in this decade have occurred at the Flores and Wetar thrusts. The $M_w = 7.9$ December 1992 Flores earthquake is the latest and largest of many to occur along the backarc thrusts.

Preliminary GPS results show that the slip rate associated with backarc thrusting increases from Bali eastward to about 50 mm a^{-1} at the eastern end of the Flores thrust and reaches the full expected rate of Australia–Eurasia relative motion (70 mm a^{-1}) at the Wetar thrust north of Timor (Genrich *et al.* 1994). GPS appears to be confirming the inference based on earthquakes (McCaffrey 1988) and crustal structure (Silver *et al.* 1983) that the eastern Sunda arc is rotating anticlockwise about a pole in eastern Java.

Timor appears to be moving northward relative to the Sunda Shelf (SEA) at about the same rate as Australia, suggesting that the Timor trough no longer accommodates subduction (Johnston & Bowin 1981; McCaffrey & Abers 1991; Genrich *et al.* 1994). The northward motion of the extinct volcanic islands north of Timor is revealed with GPS to be similar to that of southern Timor (Genrich *et al.* 1994); hence, little of the northward motion of Australia is now accommodated by internal deformation of the Banda arc structure. The island arc structure, bounded by the Timor trough and the Wetar backarc thrust, is rigidly thrusting over the backarc basin. The present geometry is probably quite young; the Wetar thrust exhibits less than 10 km of shortening (McCaffrey & Nabelek 1986), which would take only 0.15 Ma at the present rate of 60 mm a^{-1}. Probably between 3 Ma, when collision began, and 0.15 Ma convergence was in part accommodated by shortening and thickening of the forearc (Snyder *et al.* 1993). The Sunda arc now shows a gradual transition from subduction of oceanic lithosphere south of Java to a completed accretion of an island arc terrane to a continental margin at Timor. In the process, convergence has jumped from the forearc trench to the backarc thrust.

South of Timor, the Timor trough trends about N70°E while the plate convergence vector is probably close to N10°E (Tregoning *et al.* 1994), resulting in an obliquity of about 30° (Fig. 4a). The geometry predicts that the Timor forearc should be under ENE-trending, left-lateral shear and possibly arc-parallel tension. Interplate earthquake slip vectors (Fig. 5a) are too few to confirm this; values of v_s inferred from slip vectors range from zero to the full arc-parallel motion rate (Fig. 4a). The few available slip vectors show motions both parallel to plate convergence and perpendicular to the trench (Fig. 5a), suggesting a complex spatial variation in slip partitioning (below we see that this bimodal distribution of slip vectors is common at forearcs with large curvature). Recent earthquakes in the overriding plate suggest that both shearing and

stretching are occurring. In particular, two shallow earthquakes beneath Timor show left-lateral, strike-slip on NE-trending, vertical planes and shallow, N-striking, normal faulting events are found north of central Timor (Fig. 5a) (McCaffrey 1988). GPS results also suggest that slow E–W stretching of the arc may occur (Genrich *et al.* 1994).

New Guinea

The island of New Guinea accommodates oblique convergence between the Pacific and Australian plates at a rate of about 12 cm a^{-1} (Fig. 5b) and azimuth of N70°E. The young, high mountain belt, called the Highlands fold-and-thrust belt, trends at N100°E, so is about 60° away from being perpendicular to plate convergence. Large earthquakes suggest that shortening and shear are distributed over much of the island (Abers & McCaffrey 1988; McCaffrey & Abers 1991; Fig. 5b). Earthquakes within the Highlands are predominantly thrust and strike-slip with strikes generally parallel to structure rather than perpendicular to the plate convergence direction (Fig. 6a). Oblique convergence within the Highlands belt of Irian Jaya is therefore largely partitioned. The Mamberambo thrust belt (Fig. 5b) shows many more earthquakes with planes that strike perpendicular to the plate vector, suggesting less partitioning there (Fig. 6b).

Recent GPS measurements (Puntodewo *et al.* 1994) reveal less than 2 cm a^{-1} of shortening and less than 3 cm a^{-1} of left-lateral shear between sites at the north and south coasts of E Irian Jaya (at about 140°E) even though nearly 6 cm a^{-1} of shortening and 10 cm a^{-1} of left-lateral shear are predicted by Pacific–Australia relative motion. At the longitude of central New Guinea, most of the motion between Australia and the Pacific occurs offshore, probably at the New Guinea trench, contrary to inferences made from geology and seismology.

In westernmost New Guinea, plate motion appears to be accommodated in a different manner. GPS sites on the Bird's Head appear to move relative to Australia at nearly the same rate as the Pacific (Puntodewo *et al.* 1994; Stevens *et al.* 1995). In the vicinity of the Bird's Head, the majority of Pacific–Australia motion occurs by large-scale WSW motion of the Bird's Head relative to Australia. The fault (or faults) on which this motion occurs is not clear although in the SW the main boundary is probably the Tarera–Aiduna fault (Hamilton 1979; Abers & McCaffrey 1988). Manuel Pubellier (pers. comm. 1994) suggests that a large, NE-trending shear zone exists landward of the east coast of Cenderwasih Bay (Fig. 5b). If so, it could be among the fastest slipping continental

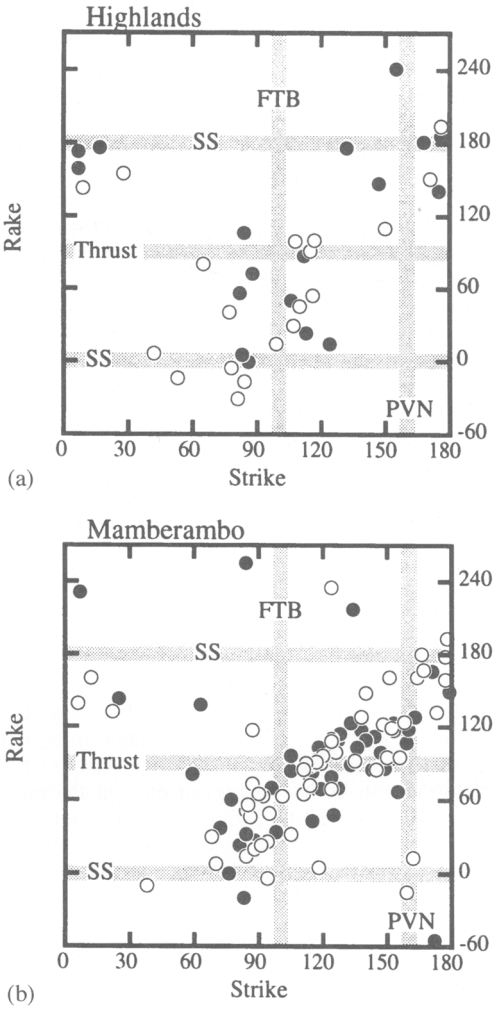

Fig. 6. Plot of rake angles vs. strike angles for earthquakes in (**a**) the New Guinea fold-and-thrust belt (FTB) between 135° and 144°E and (**b**) the Mamberambo thrust belt. For each event, both nodal planes are shown (using open and closed circles). The vertical line labelled FTB shows the trend of the fold-thrust belt, and PVN shows the trend perpendicular to the plate convergence direction. Rake angles near 90° indicate thrusting and those near 0° and 180° degrees are strike-slip (SS). Events with a strike near 100° and rake near zero reveal left-lateral slip on a plane parallel to the FTB.

shear zones in the world, being at least 7 cm a^{-1} (Stevens *et al.* 1995). The Sorong fault, at least where it passes through the Bird's Head, cannot now form the main boundary between the Pacific and Australia because GPS sites on opposite sides

of the fault show little relative motion (Puntodewo *et al.* 1994).

In Papua New Guinea (PNG), the Huon–Finisterre (HF) arc terrane is being emplaced onto the Australian continent along a north-dipping thrust fault that crops out in or near the Markham Valley (MV) (Fig. 5b). Slip vectors of thrust earthquakes beneath the HF range north of the valley remain perpendicular to the valley as it swings to a NW trend (Fig. 5b). This rotation of the slip vectors cannot be explained by a single pole of rotation between rigid plates north and south of the valley. Schouten & Benes (1996) argue that the rotation of the slip vectors is caused by rapid deformation south of the New Britain trench and MV. On the bases of geological observations (Abbott *et al.* 1994), microearthquakes (Kulig *et al.* 1993), and large earthquakes (Abers & McCaffrey 1994), it is interpreted that the HF range is cut by cross-faults that accommodate relative slip and rotations of blocks of the HF range as it moves southward. In the case of the HF block, slip partitioning is accommodated by faulting at high angles to the trench as in Cascadia and the Aleutians, rather than arc-parallel faults, as in Sumatra.

Solomons and New Hebrides

The Solomon and New Hebrides trenches form the boundary between the Pacific and Australian plates and, due to their great curvature, are the sites of large variations in convergence obliquity. The deviations of slip vectors from the plate vectors suggest that both forearcs deform significantly and partition the slip between the plates. At the southern end of the New Hebrides trench, west of 173.5°E, slip is partitioned completely so that thrust earthquakes at the trench have their slip vectors perpendicular to the trench and nearly perpendicular to the plate convergence vector (Fig. 7a). Going west around the bend in the trench, the slip vectors remain perpendicular to the trench to 18°S where the trench becomes nearly normal to the plate vector. East of about 173.5°E, the slip vectors rotate so that they form an angle of about 45° to the trench and plate vector. The extensional strain rate estimated for the southern New Hebrides forearc from the slip vectors is $12.3 \pm 2.5 \times 10^{-8}$ a^{-1} (Fig. 4c).

The Solomon trench becomes nearly parallel to the plate vector at the San Cristobal section (Fig. 7b). Slip vectors for earthquakes between 162° and 165°E show two orientations: one nearly perpendicular to the local trend of the trench and the other nearly parallel to the plate vector. If partitioning occurred by a detached forearc sliver moving along the arc, then the events with slip vectors perpendicular to the trench would be closer to the trench (i.e. below the translating sliver) than those showing oblique slip. The uncertainties in the epicentral locations of these events preclude discerning such a pattern. Nevertheless, structures accommodating shearing and thrusting must be within a few tens of kilometres (the uncertainties in epicentres) of each other. Some fault plane solutions (Fig. 7b) show left-lateral, strike-slip faulting on E–W orientated, nearly vertical faults; these faults are consistent with the type needed to partition the slip by a small sliver of the forearc being translated eastward at a high rate relative to the arc.

Tonga trench

According to the NUVEL-1A Pacific–Australia pole of rotation, the Pacific plate subducts beneath the Tonga arc in a direction nearly perpendicular to the trend of the trench throughout most of its length (Fig. 1b), although the obliquity gets large at the northern and southern ends (Fig. 4d). Earthquake slip vectors at the Tonga trench from 15°S to 35°S, deviate by 20° or less from the NUVEL-1A Pacific–Australia plate vector (Fig. 8a). If this pole applies to the Tonga trench then slip vectors suggest that the southern Tonga forearc translates very slowly (10 mm a^{-1} on average), left-laterally relative to Australia and does so as a rigid block (Fig. 4d; Table 1).

GPS measurements by Bevis *et al.* (1995) suggest that the northern Tonga forearc rotates rapidly away from Australia as a rigid block (Fig. 1b). Slip vectors also suggest that the forearc is rigid as they can be matched throughout most of the length of the island arc with a single pole of rotation at 54°S, 173°E (Fig. 8a). However, the poles of rotation estimated from GPS and from slip vectors are quite distant. The 3 GPS vectors (relative to fixed Pacific plate) from Tonga forearc sites are all matched within 2 mm a^{-1} in rate and 2° in azimuth by a pole at 32.6°S, 178.9°W (Fig. 1b), and an angular velocity of –7.1° Ma (the distance from the pole to the observation points is constrained by the gradient in GPS velocities). This pole falls near the central Tonga trench (Fig. 1b) and therefore cannot describe the motion of the entire forearc from north to south because it predicts spreading between the forearc and the Pacific south of 33°S. There is probably a structure within the forearc south of the GPS sites that separates the N and S sections of the forearc. Most probably this boundary is near 24°S where the Louisville Ridge intersects the trench and spreading in the Lau Basin appears to terminate (Fig. 1b).

The northern Tonga arc goes through a large bend until the trench is nearly parallel to plate

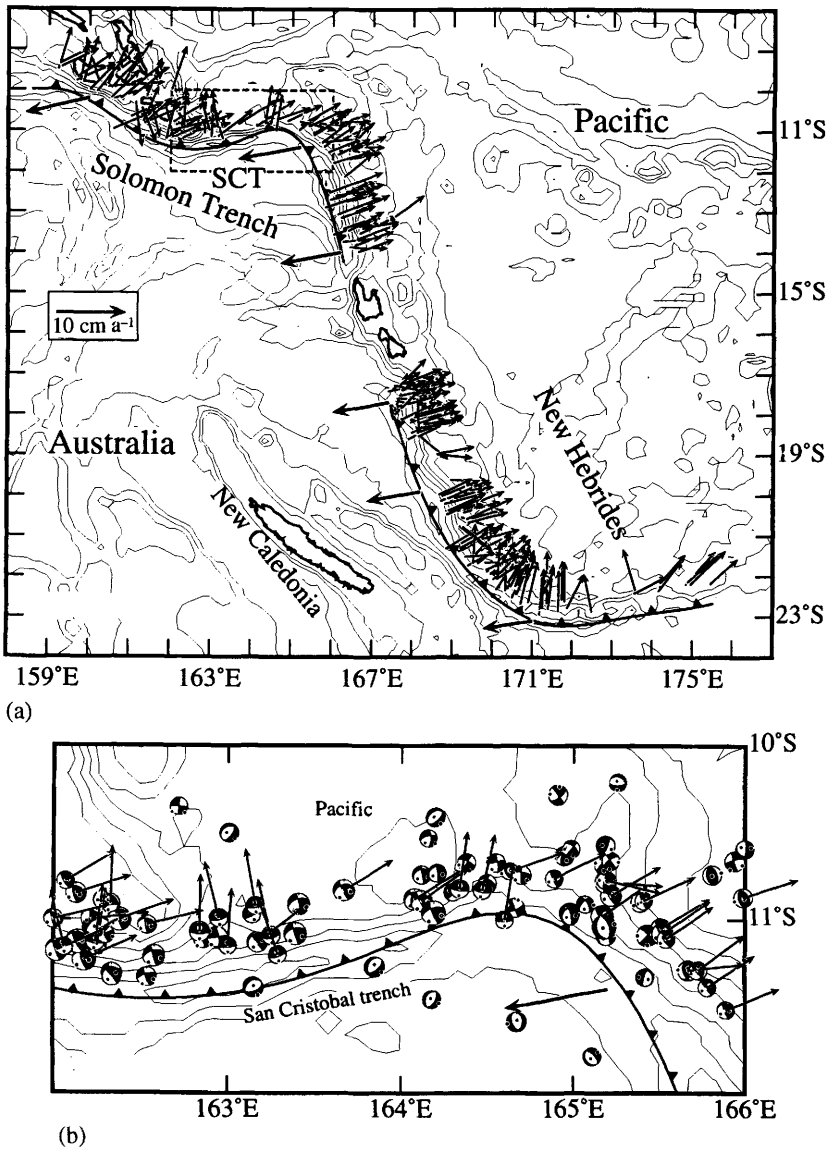

Fig 7. (**a**) Map of earthquake slip vectors (small arrows) and plate convergence vectors (large arrows) based on Pacific-Australia pole (DeMets *et al.* 1994*a*) at the Solomon and New Hebrides arcs. SCT, San Cristobal trench. Dashed outline box shows area of b. (**b**) Map of earthquake mechanisms (Harvard CMT 1977–1994; $M_s \geq 5.0$) and slip vectors at the San Cristobal trench. The large arrow shows the convergence between Australia and the Pacific.

convergence (Fig. 8b), in the same fashion as the southern New Hebrides, San Cristobal, and southern Marianas arcs. Like the San Cristobal trench, slip vectors at the northern Tonga forearc appear to describe two sets of directions; parallel to the plate vector and perpendicular to the trench (Fig. 8b). The averages of these slip vectors imply a rapid arc-parallel extensional strain rate (Table 1; Fig. 4d) for the northern Tonga forearc. However, because the trench-normal slip vectors are arcward (SW) of the vectors that parallel plate motion (Fig. 8b), they probably occur either within the subducted slab or in the upper plate and are not indicative of the interplate slip direction. (If this

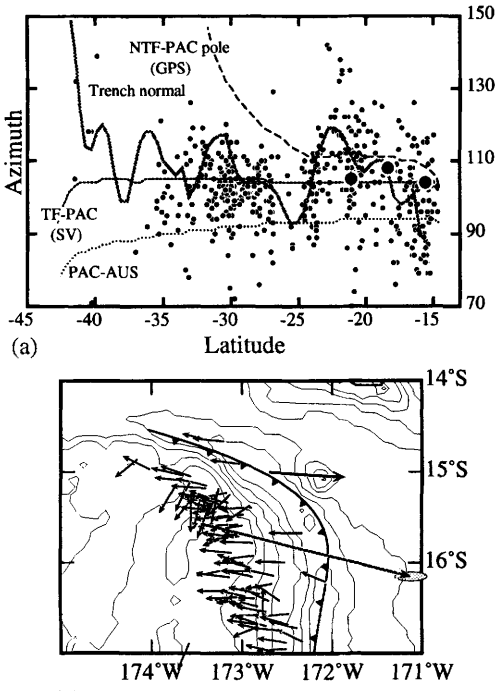

Fig. 8. (**a**) Plot of slip vector azimuths (small dots), GPS vector azimuths (large dots), the azimuth normal to the Tonga trench, the Pacific–Australia plate convergence direction (PAC–AUS), and the directions predicted by a pole of rotation between the north Tonga forearc and the Pacific based on GPS vectors (labelled GPS) (Bevis et al. 1995) and by a pole based on slip vectors (labelled SV). (**b**) Map of earthquake slip vectors (small, black arrows) beneath the northern Tonga forearc, the Pacific–Australia predicted direction (large, black arrow = 84 mm a^{-1}) and the GPS vector (grey arrow = 240 mm a^{-1}).

rotation of the slip vectors resulted from a detached sliver, these events should be trenchward, NE, of the vectors that parallel plate motion.) Excluding these southerly trending slip vectors results in a near zero arc-parallel strain rate for the northern Tonga forearc, in agreement with GPS results of Bevis *et al.* (1995).

Slip vectors east of northern New Zealand reveal a large degree of slip partitioning and v_s values suggest approximately 30 mm a^{-1} of right-lateral shear across the North Island, in agreement with geodetic measurements (Fig. 4d) (31 ± 9 mm a^{-1} from Walcott 1984). In the South Island the plate vector becomes nearly parallel to the island and most of the motion occurs by oblique slip near the Alpine fault, although there is still a small convergent component taken up by thrusting on faults parallel to the Alpine fault (Anderson *et al.* 1993).

Philippines

The Philippines are a second region that Fitch (1972) regarded as revealing slip partitioning – between the Philippine trench and the left-lateral Philippine fault. Using the Seno *et al.* (1993) PSP–Eurasia pole, the Philippine fault and trench system appears to be strongly partitioned (Barrier *et al.* 1991) (Fig. 4e). A difficulty in the kinematic analysis of the Philippines is the lack of a reliable plate convergence vector because the presence of several faults in the Philippines makes it unlikely that the Philippine islands are rigidly attached to Eurasia. A pole of rotation can be found between the forearc and the PSP that fits the Philippine trench slip vectors and removes a large part of the obliquity (Fig. 4e). Hence, we cannot be sure, on the basis of slip vectors alone, that the Philippines are partitioned.

From combined trilateration and GPS, Duquesnoy *et al.* (1994) estimate a left-lateral slip rate on the Philippine Fault near 11°N of 26 ± 10 mm a^{-1}, which is consistent with the estimates of v_s (Fig. 4e) based on the Philippine Sea–Eurasia pole of rotation (Seno *et al.* 1993). Hence, this first reliable slip rate for the Philippine fault supports the case for the Philippine system being largely partitioned. The arc-parallel strain rate for the Philippine forearc is poorly determined as the v_s values do not vary smoothly with distance along the trench (Table 1; Fig. 4e).

Ryukyu trench

Slip vectors along the Ryukyu trench generally follow the Seno *et al.* (1993) PSP–Eurasia pole (Fig. 4f) and very little slip partitioning is evident even where the obliquity is high. If there is any arc-parallel slip of the forearc, it is of the order of 10 mm a^{-1} or less. Near the centre of the Ryukyu trench (near 28°N), slip vectors are about 30° away from the plate vector even thought the obliquity is near zero (Fig. 4f). In this region the Oki Daito Ridge hits the trench (Fig. 1a) and probably causes the local deflection of slip vectors (these two points were excluded from estimates of strain rates).

Izu–Mariana trench

Although the convergence direction is poorly known, the Marianas forearc shows strong partitioning in that slip vectors remain nearly perpendicular to the trench despite large changes in

the obliquity (Figs 4g and 9). As observed at other trenches, at the south end of the Marianas trench there appears to be two groups of slip vector directions; one nearly perpendicular to the trench and another, comprising only 2 events, that is much more oblique (Fig. 9). The values of v_s at the Mariana forearc are generally equal to v_p (Fig. 4g), indicating that the upper plate absorbs all of the arc-parallel component of plate motion by shear resulting in rapid arc-parallel extension (Table 1; Fig. 4g). At the Izu arc, the slip vectors are similar to the plate vector and no arc-parallel motion is required.

Conclusions

Earthquake slip vectors at convergent margins of SE Asia are used to infer the degree of partitioning of slip on margin-parallel and margin-normal structures. Where independent geological or geodetic estimates are available, slip vector-derived estimates of arc-parallel forearc slip rates appear accurate. Regions where oblique convergence is strongly partitioned are the Himalaya, Marianas, New Hebrides, Philippines, Sumatra, Markham Valley, and New Zealand. At some strongly curved margins, earthquake slip vectors are bimodally distributed between the convergence direction and the trench-normal direction, suggesting that slip partitioning occurs at small spatial scales. Several forearcs reveal arc-parallel deformation even where subduction is normal to the trench, showing that subduction is a three-dimensional process.

I thank Tony Barber for many years of good work and cheer, the organizers of the symposium for allowing me to attend, and J. Milsom and D. Snyder for helpful reviews. Supported by NSF grants EAR-9105050 and EAR-9406917.

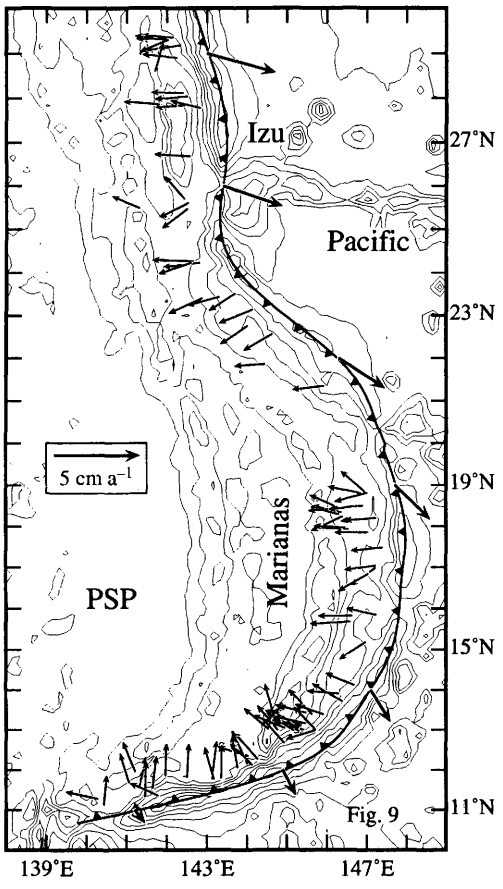

Fig. 9. Map of earthquake slip vectors (small, black arrows) beneath the Izu–Mariana forearc, and the PSP–Pacific (Seno *et al.* 1993) predicted directions (large, black arrows).

References

ABBOTT, L. D., SILVER, E. A. & GALEWSKY, J. 1994. Structural evolution of a modern arc-continent collision in Papua New Guinea. *Tectonics*, **13**, 1007–1034.

ABERS, G. & MCCAFFREY, R. 1988. Active deformation in the New Guinea Fold-and-Thrust Belt: seismological evidence for strike-slip faulting and basement-involved thrusting. *Journal of Geophysical Research*, **93**, 13 332–13 354.

—— & —— 1994. Active arc-continent collision: Earthquakes, gravity anomalies and fault kinematics in the Huon–Finisterre collision zone, Papua New Guinea. *Tectonics*, **13**, 227–245.

ANDERSON, H., WEBB, T. & JACKSON, J. 1993. Focal mechanisms of large earthquakes in the South Island of New Zealand: implications for the accommodation of Pacific-Australia motion. *Geophysical Journal of the Royal Astronomical Society*, **115**, 1032–1054.

BARRIER, E., HUCHON, P. & AURELIO, M. 1991. Philippine Fault: A key for Philippine kinematics. *Geology*, **19**, 32–35.

BELLIER, O., SEBRIER, M. & PRAMUMIJOYO, S. 1991. La grande faille de Sumatra: geometrie, cinematique et quantite de deplacement mises en evidence par l'imagerie satellitaire. *Comptes Rendus de l'Académie des Sciences de Paris*, **312**, 1219–1226.

BEVIS, M., TAYLOR, F. W., SCHUTZ, B. E., RECY, J., ISACKS, B. L. *ET AL.* 1995. Geodetic observations of very rapid convergence and back-arc extension at the Tonga island arc. *Nature*, **374**, 249–251.

CURRAY, J. R. 1989. The Sunda Arc: A model for oblique plate convergence. *In:* VAN HINTE, J. E., VAN WEERING, TJ. C. E. & FORTUIN, A. R. (eds) *Proceedings. Symposium Snellius-II Expedition, Jakarta, Nov. 23–28, 1989, Vol. 1, Geology and Geophysics of the Banda Arc and Adjacent Areas.* Netherlands Journal of Sea Research, **24**, 131–140.

——, MOORE, D. G., LAWVER, L. A., EMMEL, F. J., RAITT, R.W., HENRY, M. & KIECKHEFER, R. 1979. Tectonics of the Andaman Sea and Burma. *In*: WATKINS, J. S., MONTADERT, L. & DICKERSON, P. W. (eds) *Geological and Geophysical Investigations of Continental Margins.* AAPG Memoir, **29**, 189–198.

DARDJI, N., VILLEMIN, T. & RAMPNOUX, J.-P. 1991. Cenozoic fault systems and paleostress along the Cimandiri fault zone, west Java Indonesia. *In*: PRASETYO, H. & SANTOSO (eds) *The Silver Jubilee: Symposium on the dynamics of subduction and its products.* Proceedings LIPI Yogjakarta, 233–253.

DEMETS, C., GORDON, R. G., ARGUS, D. F. & STEIN, S. 1994*a*. Effects of recent revisions to the geomagnetic reversal time scale on estimates of current plate motions. *Geophysical Research Letters*, **21**, 2191–2194.

——, —— & VOGT, P. 1994*b*. Location of the Africa–Australia–India triple junction and motion between the Australian and Indian plates: results from an aeromagnetic investigation of the Central Indian and Carlsberg ridges. *Geophysical Journal International*, **119**, 893–930.

DIAMENT, M., DEPLUS, C., HARJONO, H., LARUE, M., LASSAL, O., DUBOIS, J., & RENARD, V. 1990. Extension in the Sunda Strait (Indonesia): a review of the Krakatau programme. *Oceanologica Acta*, **10**, 31–42.

——, HARJONO, H., KARTA, K., DEPLUS, C., DAHRIN, D. *ET AL.* 1992. Mentawai fault zone off Sumatra: a new key to the geodynamics of western Indonesia. *Geology*, **20**, 259–262.

DUQUESNOY, TH., BARRIER, E., KASSER, M., AURELIO, M., GAULON, R. *ET AL.* 1994. Detection of creep along the Philippine Fault: First results of geodetic measurements on Leyte island, central Philippine. *Geophysical Research Letters*, **21**, 975–978.

EKSTRÖM, G. & ENGDAHL, E. R. 1989. Earthquake source parameters and stress distribution in the Adak Island region of the central Aleutian Islands, Alaska. *Journal of Geophysical Research*, **94**, 15 499–15 519.

FITCH, T. J. 1972. Plate convergence, transcurrent faults and internal deformation adjacent to southeast Asia and the western Pacific. *Journal of Geophysical Research*, **77**, 4432–4460.

GEIST, E. L., CHILDS, J. R. & SCHOLL, D. W. 1988. The origin of summit basins of the Aleutian Ridge: Implications for block rotation of an arc massif. *Tectonics*, **7**, 327–341.

GENRICH, J., BOCK, Y., MCCAFFREY, R., CALAIS, E., STEVENS, C. *ET AL.* 1994. Kinematics of the eastern Indonesian island arc estimated by Global positioning system measurements. *EOS*, **75**, 162.

GILBERT, L., KASTENS, K., HURST, K., PARADISSIS, D., VEIS, G. *ET AL.* 1994. Strain results and tectonics from the Aegean GPS experiment. *EOS*, **75**, 116.

GOLDFINGER, C., KULM, L. D., YEATS, R. S., APPLEGATE, B., MACKAY, M. E. & MOORE, G. F. 1992. Transverse structural trends along the Oregon convergence margin: Implications for Cascadia earthquake potential and crustal rotations. *Geology*, **20**, 141–144.

HAMILTON, W. 1979. *Tectonics of the Indonesian region.* USGS Professional Paper, **1078**.

HARJONO, H., DIAMENT, M., DUBOIS, J. & LARUE, M. 1991. Seismicity of the Sunda Strait: Evidence for crustal extension and volcanological implications. *Tectonics*, **10**, 17–30.

HEGARTY, K. A., WEISSEL, J. K. & HAYES, D. E. 1983. Convergence at the Caroline-Pacific plate boundary: Collision and subduction. *In*: HAYES, D. E. (ed.) The Tectonic and Geologic Evolution of Southeast Asian Seas and Islands, Part 2. AGU Geophysical Monograph, **27**, 349–359.

HUCHON, P. & LE PICHON, X. 1984. Sunda Strait and central Sumatra fault. *Geology*, **12**, 668–672.

JARRARD, R. D. 1986. Relations among subduction parameters. *Reviews of Geophysics and Space Physics*, **24**, 217–284.

JOHNSTON, C. R. & BOWIN, C. O. 1981. Crustal reactions resulting from the mid Pliocene to Recent continent-island arc collision in the Timor region. *BMR Journal of Australian Geology & Geophysics*, **6**, 223–243.

KARIG, D. E., LAWRENCE, M. B., MOORE, G. F. & CURRAY, J. R. 1980. Structural framework of the fore-arc basin, NW Sumatra. *Journal of the Geological Society, London*, **137**, 77–91.

KULIG, C., MCCAFFREY, R., ABERS, G. A. & LETZ, H. 1993. Shallow seismicity of arc-continent collision near Lae, Papua New Guinea. *Tectonophysics*, **227**, 81–93.

MALOD, J. A., KARTA, K, BESLIER, M. O. & ZEN, M. T. 1996. From normal to oblique subduction: Tectonic relationships between Java and Sumatra. *Journal of SE Asian Earth Science*, **12**, 85–93.

MATSUZAKA, S., TOBITA, M., NAKAHORI, Y., AMAGAI, J. & SUGIMOTO, Y. 1991. Detection of Philippine Sea plate motion by very long baseline interferometry. *Geophysical Research Letters*, **18**, 1417–1419.

MCCAFFREY, R. 1988. Active tectonics of the eastern Sunda and Banda arcs. *Journal of Geophysical Research*, **93**, 15 163–15 182.

—— 1991. Slip vectors and stretching of the Sumatran forearc. *Geology*, **19**, 881–884.

—— 1992. Oblique plate convergence, slip vectors, and forearc deformation. *Journal of Geophysical Research*, **97**, 8905–8915.

—— 1994. Global variability in subduction thrust zone-forearc systems. *Pure and Applied Geophysics*, **141**, 173–224.

——. & ABERS, G. A. 1991. Orogeny in arc-continent collision: the Banda arc and western New Guinea. *Geology*, **19**, 563–566

——. & NABELEK, J. 1986. Seismological evidence for shallow thrusting north of the Timor trough. *Geophysical Journal of the Royal Astronomical Society*, **85**, 365–381.

MCKENZIE, D. & JACKSON, J. 1983. The relationship between strain rates, crustal thickening, paleomagnetism, finite strain, and fault movements within a deforming zone. *Earth and Planetary Science Letters*, **65**, 182–202.

MOLNAR, P. & LYON-CAEN, H. 1989. Fault plane solutions of earthquakes and active tectonics of the Tibetan

Plateau and its margins. *Geophysical Journal International*, **99**, 123–153.

——, ENGLAND, P. & MARTINOD, J. 1993. Mantle dynamics, uplift of the Tibetan Plateau, and the Indian monsoon. *Review of Geophysics*, **31**, 357–396.

MOUNT, V. S. & SUPPE, J. 1987. State of stress near the San Andreas fault: Implications for wrench tectonics. *Geology*, **15**, 1143–1146.

PLATT, J. P. 1993. Mechanics of oblique convergence. *Journal of Geophysical Research*, **98**, 16239–16256.

PUNTODEWO, S. S. O., MCCAFFREY, R., CALAIS, E., BOCK, Y., RAIS, J. *ET AL.* 1994. GPS measurements of crustal deformation within the Pacific–Australia plate boundary zone in Irian Jaya, Indonesia. *Tectonophysics*, **237**, 141–153.

RANKEN, B., CARDWELL, R. K. & KARIG, D. E. 1984. Kinematics of the Philippine Sea Plate. *Tectonics*, **3**, 555–575.

SCHOUTEN, H., & BENES, V. 1996. Post-Miocene collision of Australia and the Bismarck arc, western equatorial Pacific. *Earth and Planetary Science Letters*, in press.

SENO, T., STEIN, S. & GRIPP, A. 1993. A model for the motion of the Philippine Sea plate consistent with NUVEL-1 and geological data. *Journal of Geophysical Research*, **98**, 17 941–17 948.

SIEH, K., ZACHARIASEN, J., BOCK, Y., EDWARDS, L., TAYLOR, F. & GANS, P. 1994. Active tectonics of Sumatra. *GSA Abstracts with Programs*, **26**, A-382.

SILVER, E. A., REED, D., MCCAFFREY, R., & JOWODIWIRYO, Y. 1983. Back-arc thrusting in the eastern Sunda Arc, Indonesia: a consequence of arc-continent collision. *Journal of Geophysical Research*, **88**, 7429–7448.

SNYDER, D. B., PRASETYO, H., TJOKROSAPOETRO, S., BLUNDELL, D. J., BARBER, A. J., RICHARDSON, A. N. & MILSOM, J. 1993. A deep seismic reflection transect across the youngest mountain range in the world, the active convergent margin between the Australian craton and the Banda volcanic arc near Timor, Indonesia. *EOS*, **74**, 444.

STEVENS, C., PUNTODEWO, S. S. O., MCCAFFREY, R., BOCK, Y. & CALAIS, E. 1995. Out of the pot and into the frying pan: A Bird's Head's view of tectonic escape. *International Union of Geodesy and Geophysics, XXI General Assembly*, p. A38.

TREGONING, P., BRUNNER, F. K., BOCK, Y,. PUNTODEWO, S. S. O., MCCAFFREY, R. *ET AL.* 1994. First geodetic measurement of convergence across the Java Trench. *Geophysical Research Letters*, **21**, 2135–2138.

WALCOTT, R. I. 1984. The kinematics of the plate boundary zone through New Zealand: a comparison of short- and long-term deformations. *Geophysical Journal of the Royal Astronomical Society*, **79**, 613–633.

WEISSEL, J. K. & ANDERSON, R. N. 1978. Is there a Caroline plate? *Earth and Planetary Science Letters*, **41**, 143–158.

YU, S.-B. & CHEN, H.-Y. 1994. Global positioning system measurements of crustal deformation in the Taiwan arc-continent collision zone. *Terrestrial, Atmospheric and Oceanic Sciences* **5**(4), 477–498.

ZWICK, P. & MCCAFFREY, R. 1991. Seismic slip rate and direction of the Great Sumatra Fault based on earthquake fault plane solutions. *EOS*, **72**, 201.